Extended hydrologic impacts of karst discharge zone confinement - a modeling study

Marc Ohmer[1], **Tanja Liesch**[1], **and Nico Goldscheider**[1]

[1]**Institute of Applied Geosciences, Division of Hydrogeology, Karlsruhe Institute of Technology, Karlsruhe, Germany**

ABSTRACT

Karst springs are the natural outflow of karst water to the surface. These springs occur where the water table can reach the surface unimpeded. This study examines the effect of alluvial deposits with varying thickness and permeability, covering the main outlet (karst spring) of a karst network on karst drainage (e.g., development of the karst water, drainage patterns, conduit-matrix interaction) as a result of a positive base level shift. This was realized with a numerical conceptual model (FEFLOW) of a hypothetical karst aquifer with 6 model configurations (inactive vs. active conduit flow, free vs. confined spring conditions with 20 m and 50 m sediment cover, respectively, with low and high hydraulic conductivity). Conduit flow and coupled conduit-matrix interactions were incorporated into the model with one-dimensional discrete feature elements. The results show that the permeability of the sediments has a more distinctive effect on conduit discharge than their thickness. The conduit network significantly contributes to the drainage even with a fully confined spring outlet. The conduit system acts as a water collector from the matrix in the recharge zone. The buried outlet increases the hydrostatic pressure farther along the conduit, and water is pushed upwards back into the matrix in the vicinity of the stratigraphic contact. Depending on the depositional setting, this results in the evolution of one to multiple new flow systems towards new potential spring sites. The results obtained here provide insight into the likely responses of natural karst systems.

Keywords: Karst modelling, discrete feature element approach, confined karst spring, base-level rise

1 INTRODUCTION

In addition to their role as an essential worldwide water resource, karst areas hold a variety of natural resources and provide critical ecosystem functions (Goldscheider, 2019). The evolution of a karst system is closely linked to the temporal development of the regional base level as it guides the regional orientation of the runoff pattern and controls the main flow gradient. A mature karst system with fast flow in conduits and caves towards major karst springs can develop if the base level is stable over a long period. Extremely abrupt changes to the boundary conditions are brought by geomorphologically rapid events (often combined with climatic changes). For example, active tectonic processes can cause a rapid shift of the base level and changes in the denudation rates (Ford and Williams, 2007). Negative base level

shifts resulting from tectonic uplift, sea-level fall, or valley deepening by glacial or fluvial erosion cause downward development and the rejuvenation of the karst network. Positive shifts can be caused by filling basins with alluvial, fluvial, lacustrine, glacial, or volcanic deposits, causing karst outlets to become covered with sediments of varying thickness and hydraulic properties. A similar situation can occur to coastal springs due to sea-level rise and the resulting increased water head (Bakalowicz, 2005) since the denser saltwater of the sea forms a barrier to the freshwater outflow.

The following is a brief outline of four karst systems that have experienced such a rapid base-level shift and have thus evolved to their present state. The most prominent large-scale example of the hydrogeological consequences of such a rapid change in groundwater level is the Messinian salinity crisis in the Miocene (Audra et al., 2004; Bakalowicz, 2005). As a result of the closure of the Strait of Gibraltar and the subsequent evaporation of seawater, the level of the Mediterranean sea dropped by up to 1500 m (Gargani and Rigollet, 2007). This extreme base-level drop led to a drastic increase in karstification in the depths of the Mediterranean karst aquifers. Rivers like the Rhone formed deep gorges. The crisis ended during the Pliocene with the Zanclean flood event caused by the erosion of the Strait of Gibraltar barrier. The resulting rapid rise in sea level led to the deposition of thick, low permeable marine and continental sediments in the paleo-valleys and the clogging of the outlets of the karst systems. This forced the water to rise through vauclusian systems to new discharge points like the eponymous **Fontaine de Vaucluse** as the best-known example.

Another example of the effects of a positive base level shift with subsequent valley aggradation is the **Presciano Spring system** (PSS). This spring system is one of the major outlets of the Meso-Cenozoic Gran Sasso fractured karst aquifer, located in the Tirino River Valley (Central Italy). The PSS is a 2000 m² seepage area forming several large limnocrenic springs at the contact zone of the Meso-Cenozoic karst and Quaternary lacustrine deposits (Fiasca et al., 2014). The springs are characterized by a relatively constant discharge, which is atypical for karst springs, and by other peculiar hydrogeological, physicochemical, hydrogeochemical, and biological characteristics that suggest a local superimposition of a dual groundwater flow system (Petitta et al., 2015; Peleg and Gvirtzman, 2010). The system consists of a fast component transported from the core of the aquifer via a subsurface karst conduit or at least a highly fractured flow path and a slow base flow path within the microfracture network.

The **Zuqim-Spring-System** (also known as Ein Feschchar-Spring) is located on the northwestern shore of the Dead Sea (which defines the base-level) close to the escarpment of the Dead Sea transform faulting system is another example. The Dead Sea fault system lowered the base level and directed the drainage system away from the Mediterranean Sea toward the Dead Sea. The spring system is draining the Albian to Turonian carbonate rocks from the Cretaceous Judea Group along a wide area of increased permeability (Burg et al., 2016). Groundwater in the uplifted Judea Group aquifer crosses the western fault of the graben eastward and discharges into the young fluvio-lacustrine, graben filling sediments of the Dead Sea Group. There it enters a complex system of subaquifers. The groundwater rises along different paths within the heterogeneous sediments, discharging at numerous springs and seepage areas. The recent rapid drop in the level of the Dead Sea led to the migration of the springs towards the current shoreline and changes in the springs'

discharge rates.

The fourth example is the **Donauried gravel aquifer** located at the geological contact of the Swabian-Franconian Alb, the most extensive karst aquifer system in Germany, and the Molasse foreland basin of the Alps. In this area, the Jurassic karst formation dips beneath the wedge-shaped Molasse, which spread northwards during the Tertiary and overlaid the paleokarst with heterogeneous, low-permeability deposits of up to several hundred meters. This led to a complex interaction between the karst aquifer, the unconsolidated gravel aquifer in the Donauried, and the Molasse, which acts as a hydraulic barrier. These various flow paths result in mixtures of multiple water components of different ages from the karst- into the gravel-aquifer reservoir (Schloz et al., 2007). A large part of the karst groundwater enters the alluvial aquifers in the Danube valley in areas where (a) the gravels lie directly on the Jurassic limestones, (b) the low permeability Molasse sediments have been eroded or are only present in minor thicknesses, and (c) vertical upwelling of karst water through fractures in the Molasse into the alluvial aquifer is possible (Kolokotronis et al., 2002). Zones of upwelling karst groundwater can be located by temperature anomalies, chemical analyses and salt dilution tests (Udluft, 2000; Fahrmeier et al., 2021, 2022).

Numerous studies present investigations of karst systems with main drainage in conduits and springs (Glennon and Groves, 2002; Bonacci, 2001; Jeannin, 2001; Chen and Goldscheider, 2014; Frank et al., 2019, e.g). Most studies have in common that they depict karst systems draining through one or more free-draining springs. In contrast, very little is known about karst systems with a sediment-covered discharge zone. Modeling groundwater flow in karst aquifers is challenging, facing many limitations due to the extreme heterogeneity of hydraulic parameters and the dual flow path regime (Scanlon et al., 2003; Kovács and Sauter, 2007). Therefore, the modeling approach, including the model complexity, varies widely as a function of the research question, depth of process representation, and, most importantly, the data availability. In lumped parameter models, physical processes are conceptually considered as a function of linear or nonlinear relationships of storage and discharge at the resolution of the entire aquifer system (Hartmann et al., 2014). This type of model is used in studies that aim to determine the dynamic response of karst discharge without consideration of spatial variability. In addition to studies that utilize reservoir models (Fleury et al., 2007; Martínez-Santos and Andreu, 2010; Shi et al., 2013; Ladouche et al., 2014), there has been a recent increase in the use of data-driven models (Paleologos et al., 2013; Lakušić, 2018; Liesch et al., 2021). Distributed karst models divide the model area into a subset with fixed hydraulic parameters. Distributed model approaches, used in karst modeling, can be categorized into (in order of investigation effort, practical applicability, and ability to simulate heterogeneities) (1) Equivalent Porous Medium Approaches (EPM) (Ghasemizadeh et al., 2015; Abusaada and Sauter, 2013), (2) Double Continuum Approaches (DC) (Kordilla et al., 2012; Bresinsky et al., 2020) and (3) Combined Discrete-Continuum approaches (CDC), which are used in this study. This approach was first applied by Kiraly (1998). The matrix is represented by a continuum formulation, while the conduits are embedded as one-dimensional discrete elements. The best-known codes that implement this approach are MODFLOW with the CFP package (Shoemaker et al., 2008), MODFLOW-USG with the CLN package

(Panday et al., 2013) as well as proprietary FEFLOW Discrete Feature Elements (DFN) (Diersch, 2014). The latter is used in this study and has been applied elsewhere (e.g Green et al., 2006; Berglund et al., 2020; Ninanya et al., 2018; Kavouri and Karatzas, 2016).

The main objective of this study is to investigate the hydraulic conditions that develop in a mature karst system when the base level rises, and thus the main spring outlets become clogged with sediments of varying hydraulic conductivity and thickness. Using a simplified three-dimensional numerical model with different model settings (with and without a sediment layer with varying thickness and permeability), this study aimed to investigate how deposits overlying the discharge zone alter the karst drainage and the structure of the groundwater flow pattern. Two specific objectives motivate the work:

- What is the effect of a discharge zone confinement or semi-confinement on flow velocities and flow rates in the conduit network, the matrix, and the conduit matrix-interaction?
- What is the influence of thickness and/or permeability of the confining cover layer for the karst drainage and its drainage patterns?

2 METHODOLOGY

2.1 Description of the model scenarios

We have developed six model configurations to investigate the hydrologic effects of discharge zone confining sediments with varying thickness and permeabilities (Fig. 1) on karst drainage (e.g., development of the karst water table, the drainage patterns, conduit-matrix interaction):

- A: Flow through the aquifer system with no karst featured added. This configuration serves as a reference to quantify the influence of the conduit networks in the other configurations.
- B: Karst drainage primarily through the main conduit network with a non-covered karst spring outlet. This variant shows the initial state before beginning the positive base level shift and the discharge zone confinement.
- C: Thin sediment cover (20 m) on the discharge zone with highly permeable unconsolidated sediments (10^{-2} m/s) such as fluvial sand to gravel deposits.
- D: Thin (20 m) sediment cover on the discharge zone with low permeable sediments (10^{-8} m/s) such as silt or loess.
- E: Thick sediment cover (50 m) of the discharge zone consisting of the highly permeable unconsolidated sediments described in C.
- F: Thick sediment cover of the discharge zone consisting of the low permeable sediments described in D.

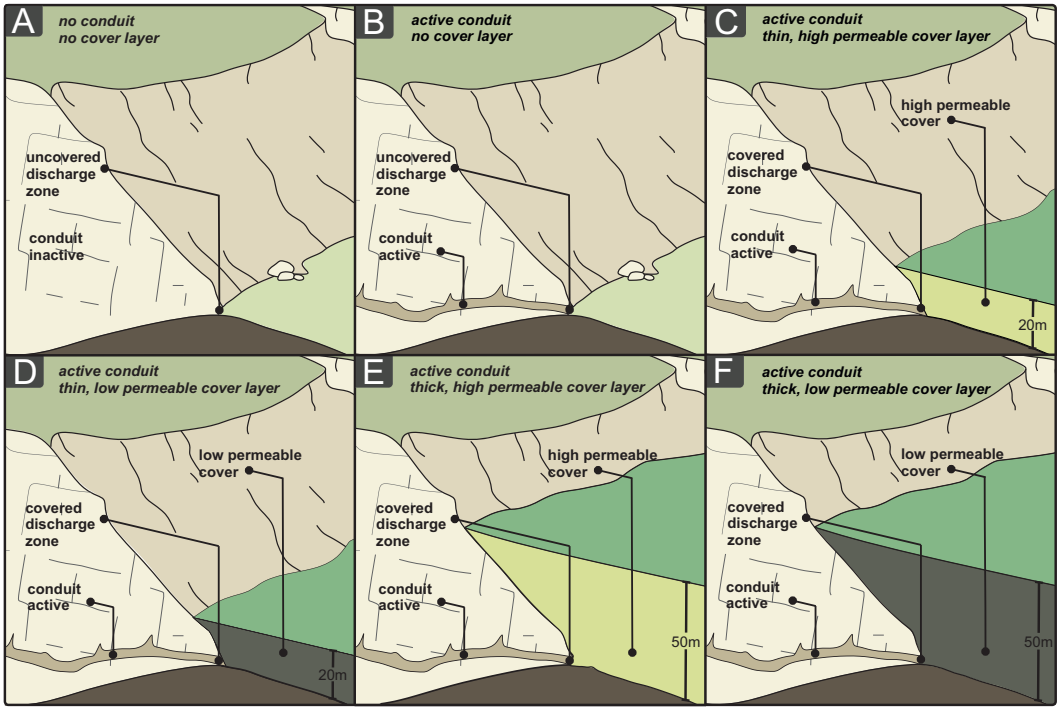

Figure 1. Schematic overview of the six model configurations (A-F) used in this study to investigate the influence of discharge zone confinement on karst drainage

.

2.2 Hydrogeological Conceptual Model

The conceptual model represents a hypothetical karst aquifer that is drained at the base level by a large perennial (fault- or dammed-) spring at the contact with an impermeable formation that acts as a barrier (Fig. 2). The spring can be characterized as a Vauclusian type. Therefore, the water emerges at the ground surface through a shaft that rises upwards at the stratigraphic boundary. The dimensions and geometry roughly correspond to those of the karst systems on the southern edge of the Swabian Alb (Villinger, 1977; Villinger and Ufrecht, 1989; Lauber et al., 2013, 2014). The spring is fed by a high-conductivity hierarchically organized karst conduit system with typical branchwork patterns. The model has a length of 21 km (length karst aquifer: 16 km) and a width of 10 km. The model was deliberately developed in a highly simplified and schematic way, neglecting a realistic karst aquifer's spatial complexity and heterogeneity, including the influence of a soil cover and the epikarst. Furthermore, it is assumed that Darcy's law governs the matrix flow. The model comprises four geological units: a karst aquifer with a matrix and a conduit conductivity, an impermeable layer below the karst layer, a sedimentary cover layer, and a drainage layer (required by the model geometry to drain the water). The karst aquifer has a constant thickness of 140 m and a catchment area of 150 km². A groundwater recharge of 200 mm/a, results in a total spring discharge rate of 0.95 m³/s. The uniform hydraulic matrix conductivity is $5 \cdot 10^{-5}$ m/s. The embedded branchwork conduit system is located at the aquifer base is divided into three sections which increase in diameter towards the outlet (I, II, III).

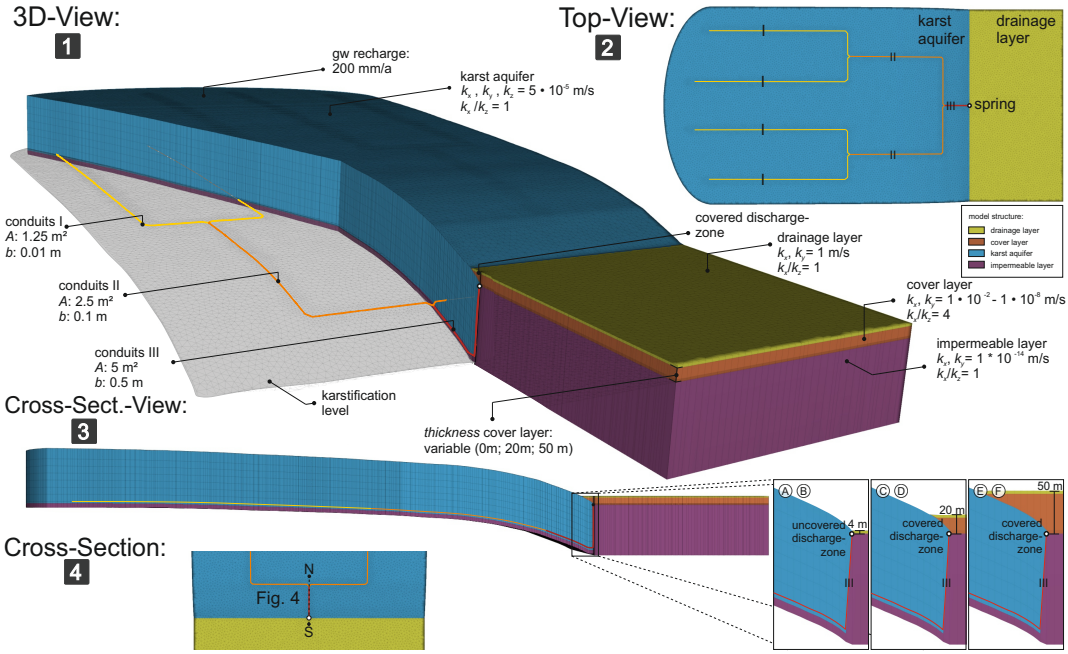

Figure 2. Schematic overview of the numerical FEFLOW model domain with all the features and the parameterization. 1: 3D view with clipping plane and view of the conduit network. 2: model domain from above. 3: Model cross-section along the main conduit, the discharge zone with different cover thicknesses of the configurations A-F. 4: Top view of the cross-section shown in Fig. 4.

2.3 Groundwater Flow Model

The groundwater flow was modeled steady-state, using the finite element, groundwater flow, and transport modeling software FEFLOW 7.3 by DHI WASY (Diersch, 2014). The model is composed of 14 slices of 455.103 elements per slice. Since the model represents a complete catchment area of the karst spring, a no-flow boundary condition was applied along the model boundary. Therefore, the total groundwater recharge (84.000 m³/d) comes entirely from recharge into the model from the top of the karst layer (groundwater recharge). The base-level was set with a specific head boundary condition according to the six configurations A-F at the height of the respective cover layer at the model outlet to represent the discharge in this elevation. The hydrodynamic and flow processes in soil, epikarst, and conduit evolution processes were neglected. The conduit flow and the conduit matrix interaction were embedded into the model with 880 discrete feature elements (DFE). These are connected 1-D and 2-D elements with increased fluid conductivity than the porous medium. DFEs are connected to the porous medium at model nodes, where they interact hydraulically with it. This approach allows the model to approximate structures such as specific faults, boreholes, tunnels, or karst channels. For the conduit network, the Hagen-Poiseuille law was iteratively chosen with apertures of 0.01 m for Section I, 0.1 m for Section II, and 0.5 m for Section III, thus providing sufficient drainage through the conduit. Still, the whole network is entirely within the phreatic zone. The governing balance equations for discrete features can be found in Diersch (2014).

3 RESULTS

3.1 Impact on Conduit Flow Rates

Fig. 3 illustrates the simulated conduit discharge in section II/III as a function of sediments' thickness and hydraulic conductivity covering the discharge zone. The left panel (1) shows the effect of a 20 m thick sediment layer, and the right panel (2) the effect of a 50 m thick cover layer. The hydraulic conductivity of the deposits were systematically reduced from 10^{-2} m/s (blue line) to 10^{-8} m/s. (red line). The black line represents the conduit discharge of the initial free-draining spring. The two middle panels give information on the locations of the conduit flow change within the model. The blue area represents the uncovered karst, and the yellow area is the karst covered by the sediments. The flow rate at a distance of 0 corresponds to the (covered) conduit outlet. The discharge of the free-draining spring is about 900 l/s, representing 90.5% of the total recharge. In the simulations with highly permeable sediments ($K = 5 \cdot 10^{-5}$ m/s), the spring discharge (seepage of water from in the deposits respectively) is reduced to 400 l/s (20 m cover layer) and 300 l/s (50 m cover layer). Sediments with a lower hydraulic conductivity cause rapid plugging of the conduit outlet

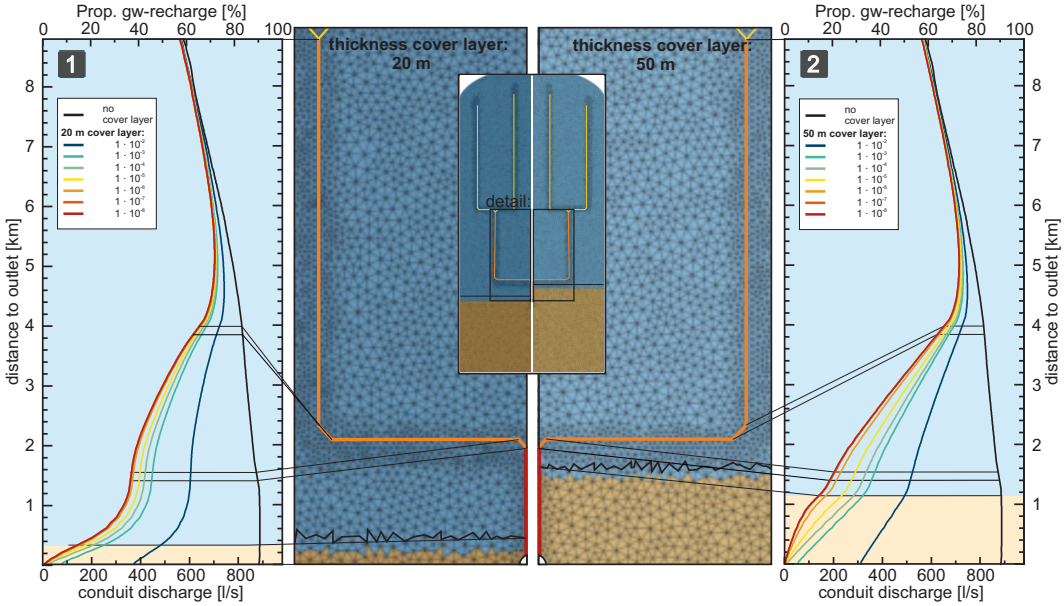

Figure 3. Discharge in conduit II/III with unaffected drainage on the outlet (black line) and with discharge zone sediment cover with thicknesses of 20 m (1) and 50 m (2). The hydraulic conductivity of the cover layer varies between 10^{-2} m/s - 10^{-8} m/s. Blue area: uncovered karst; yellow area: karst covered by deposits

with a decreasing discharge/seepage towards zero, even if the hydraulic conductivity of the cover layer is still higher than the permeability of the karst matrix ($K = 5 \cdot 10^{-5}$ m/s). For the range we examined, the permeability of the deposits has a significantly more significant effect on the conduit discharge than the thickness of the sediments. We see a linear decrease in the conduit discharge with a thick layer. For the configurations with a two-step discharge, decrease towards the outlet for the configurations with a thin layer. The most significant reduction occurs in the area where the conduit is covered by the sediments (yellow area). The effect of sediment on flow rate is evident for all configurations up to an output distance of about 7 km.

3.2 Impact on Conduit Matrix Interaction

Fig. 4 illustrates a combined line plot /cross-section view of the Darcy flux section N-S for the 6 model configurations (A-F). The Darcy flux in the conduit is shown as a red dashed line. The solid red line shows the Darcy flux in the top

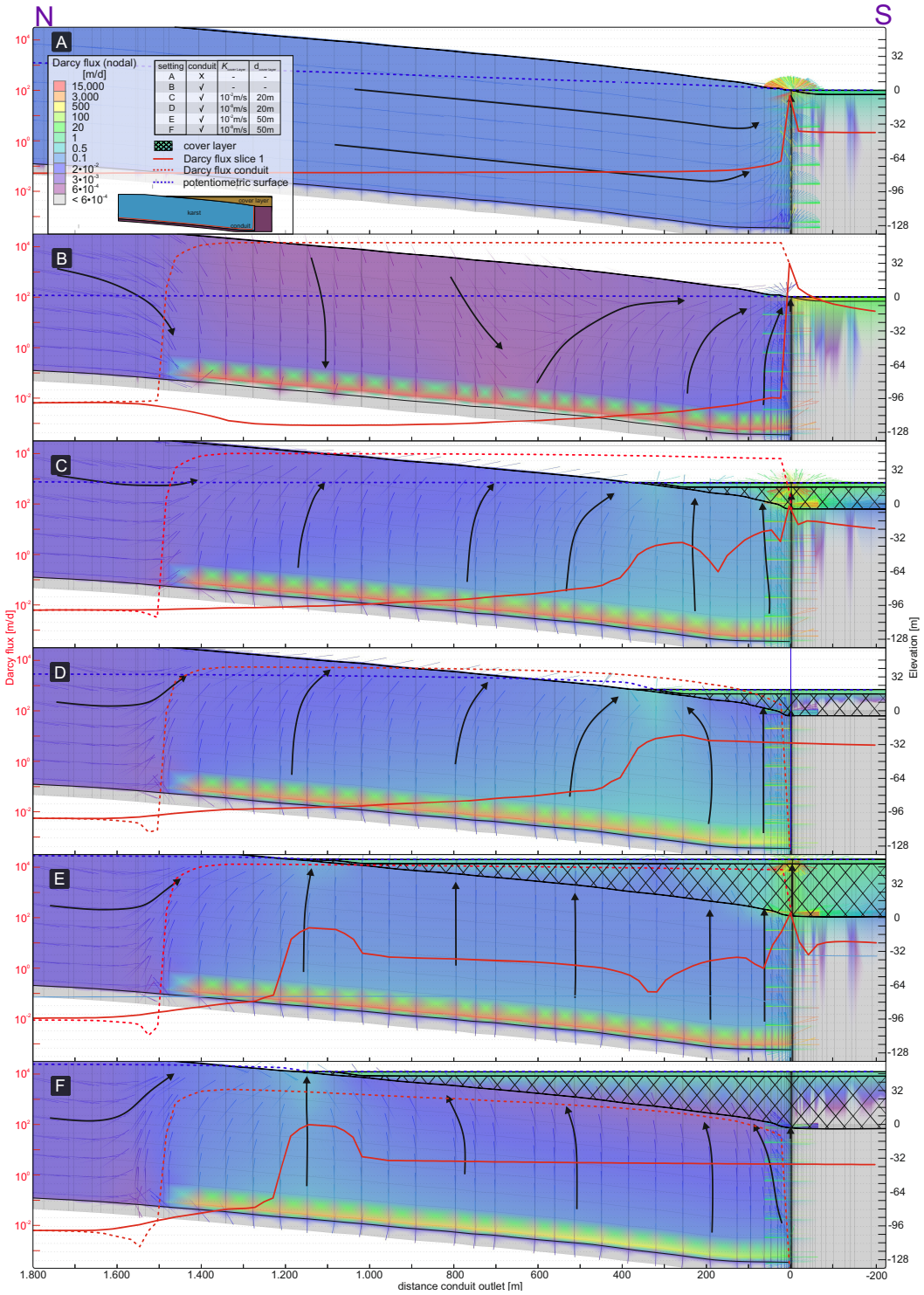

Figure 4. Nodal Darcy flux distribution along a cross-section. The solid red line represents the conduit Darcy flux in the conduit. The red dashed line is the Darcy flux in the matrix of the top model slice, and the blue line shows the potentiometric surface. Arrows display the Darcy flux flow pattern. Location of the cross-section is shown in Fig. 4

model slice. Increased flux in this slice indicates water exchange from the karst into the sediments or surface. The blue dashed line represents the potentiometric groundwater surface. Artesian conditions occur if this line is above the model surface or if the water reaches the surface. The background colors represent the Darcy flux in the conduit and the matrix in a cross-sectional view of the model domain of the 3D model. The comparison of inactive (A) and active conduit (B) systems demonstrates the central role of the conduit system in karst drainage. The conduit discharges 90.5% of the recharge (see Fig. 3). This is also shown by the significantly lower matrix flux of $9.5 \cdot 10^{-4}$ m/d compared to the setting with an inactive conduit in A with $7.5 \cdot 10^{-2}$ m/d. The flow direction changes from a slope-parallel flow (A) to a radial flow towards the conduits (B). At a horizontal distance of 600 m from the conduit outlet, the flow field changes again from gravitationally dominated downward flow towards the conduit to pressure-driven upwards flow towards the ground surface. With the increasing thickness and decreasing permeability of the deposits (C-F), the Darcy flux in the conduit decreases significantly. At the same time, more water (over a larger area) is pushed from the conduit into the matrix due to increasing water pressure within the conduits. In both configurations with a low permeable sediment cover (D, F), the water pressure led to artesian conditions within the karst layer (blue dashed line above the model surface).

3.3 Impact on Drainage Patterns

Fig. 5 shows the model domains' discharge conditions (conduit outlet, geological contact karst aquifer with sediment cover, and contact karst aquifer with the model top) for each of the six model configurations examined. The thin, high permeability layer (C) has three different flow paths to the surface result. The dominant path: 56.1% of the dammed

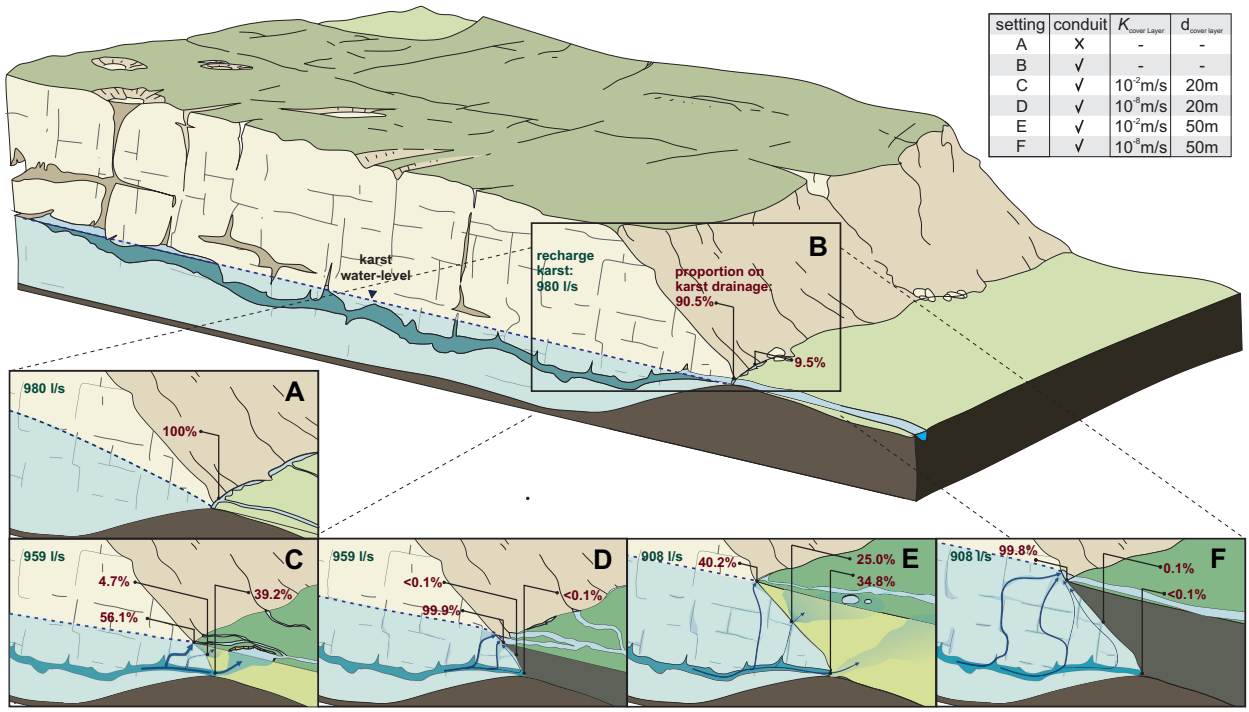

Figure 5. Influence of a cover layer (with different thicknesses and permeability) covering the drainage zone on the development of flow patterns, including the proportion of preferential flow paths in the total discharge. The difference in groundwater recharge results from the decrease in exposed karst surface area due to the sediments.

groundwater rises below the geological contact from the conduit into the matrix and seeps to the surface directly. The secondary path: 39.2% infiltrates from the reduced but still active conduit outlet into the sediments and rises vertically to the surface. A third path: the water from the conduit enters the matrix and then diffuses into the deposits (4.7%). The drainage pattern shift with increasing thickness of the cover layer (D) without change K. As the base level rises and the contact area with the sediment increases, diffuse exchange through the sediments becomes more prevalent (4.7%→25.0%). The proportion of the conduit discharge (39.2%→34.8%) decreases comparatively less than the direct discharge at the interface (56.1%→40.2%). With decreasing hydraulic conductivity of the cover layer, we see an entirely confined conduit outlet (<0.1%). There is also practically no diffusive exchange through the sediments (<0.1%). The water trapped in the conduit is forced upwards into the matrix resulting in artesian conditions near the geological contact. If fractures or fault lines are present in this zone, water will surge upwards and form an artesian spring (vauclusian-type).

3.4 Impact on Karst Water Table

The simulated steady-state potentiometric surface of the six model configurations A-F is shown in Fig. 6. In all configurations with an active conduit (B-F), the conduit acts as a dominant drainage network with strong conduit matrix interaction. The conduit acts as a drain from the surrounding matrix in section I and the upper part of section II. The gradient reverses in the further course towards the outlet, causing water to flow from the conduit into the matrix. Even for confined conditions (F), the potentiometric surface is below the level that would develop with a lower base level and without a conduit (A). In (B), the phreatic zone begins only slightly above the conduit level.

4 CONCLUSIONS

In this study, we developed a conceptual model of sediment coverage of karst outflow. We used a numerical model to investigate six different configurations to examine the impacts of sediments with varying thickness and hydraulic conductivity confining a karst discharge zone on the drainage system and drainage pattern and the conduit-matrix interaction of a karst aquifer. The results show that a thin cover of highly permeable sediments (K= 10^{-2} m/s) leads to a reduction of the conduit outlet discharge by half. With less permeable sediment cover, the conduit outlet becomes almost inactive. The influence of the permeability of the deposit cover on conduit discharge outweighs the impact of its thickness for the range of conditions examined. However, the conduit system still has a significant role in karst drainage, even with a thick and impervious cover plugging the drainage zone. The conduit collects water from the matrix in the area of the recharge zone and carries it in the direction of the confined outlet. Due to the reduced drainability of the outlet, the increased pressure in the conduit forces flow back upwards into the matrix. We see a sizeable hydraulic exchange with the karst aquifer for the thin, high permeability layer. For drainage, this results in the development of three different flow paths. First and dominant flow path: The deposits impounded the karst water level to the new rising valley floor level. Karst water seeps out at several points and forms dammed springs. In the second flow path, the water emerges from the diminished but still active buried karst cave into the sediments, rises vertically upwards within a

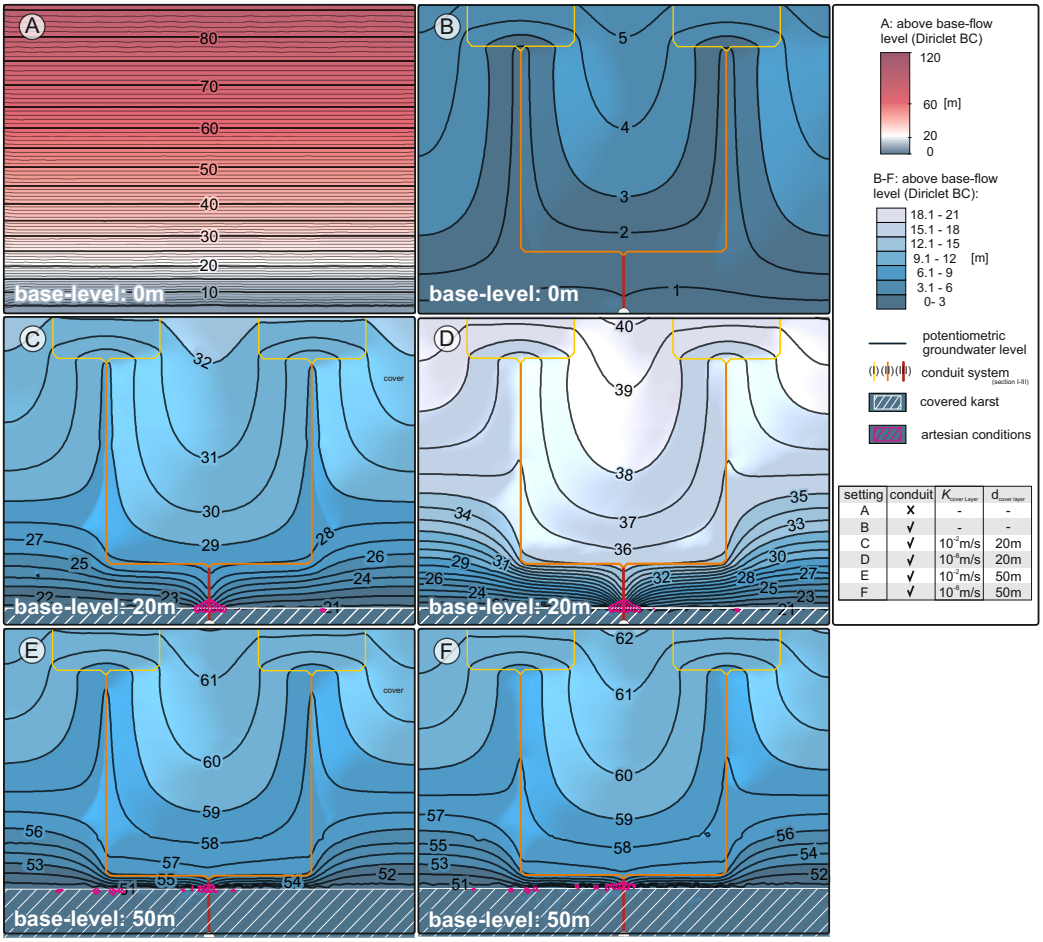

Figure 6. Simulated (steady-state) piezometric karst surface of the 6 model configurations applied in the study.

discrete zone, and appears as a big limnocrene spring. The third flow path is a superposition of the first two: impounded water passes from the conduit and interflows into the karst matrix. From there, it diffusely enters the sediments. Without changing K, more water emerges along the third flow path as the thickness increases. The results of the simulations with highly permeable sediment cover are, in many aspects, consistent with observations on the Presciano Spring System and the karst gravel-aquifer interaction in Donauried, both mentioned in the introduction part.

The highly permeable sediment cover simulation results show a significant rise of karst water from the buried conduit through the alluvial cover layer and are consistent with findings from studies on the Presciano spring system system (Petitta et al., 2015) and the karst-gravel-aquifer interaction in the Donauried (**?**), resp. support the hypotheses that buried karst conduits (or highly fractured zones) are present there.

The low permeability sediment covers form an effective hydraulic barrier. Water exchange with the sediments is negligible in such an setting and the covered spring outlet is fully confined. In the range we examined, artesian conditions occurred in the area of the geological contact. The presence of fractures or faults would then lead to a drainage reorganization. Thus, a horizontal shaft could gradually form along this zone to the new main outlet, similar to the Vaucluse spring.

5 ACKNOWLEDGMENTS

The authors would like to thank Prof. Ty Ferré for his valuable edits, suggestions, and language and grammar check. This study is a contribution to the research project Karst Aquifer Resources availability and quality in the Mediterranean Area (KARMA project, grant agreement number 01DH19022A).

REFERENCES

Abusaada, M. and Sauter, M. (2013). Studying the Flow Dynamics of a Karst Aquifer System with an Equivalent Porous Medium Model. *Ground Water*, Vol. 51, No. 4:641–650.

Audra, P., Mocochain, L., Camus, H., Gilli, , Clauzon, G., and Bigot, J.-Y. (2004). The effect of the Messinian Deep Stage on karst development around the Mediterranean Sea. Examples from Southern France. *Geodinamica Acta*, 17(6):389–400.

Bakalowicz, M. (2005). Karst groundwater: a challenge for new resources. *Hydrogeology Journal*, 13(1):148–160.

Berglund, J. L., Toran, L., and Herman, E. K. (2020). Can Karst Conduit Models Be Calibrated? A Dual Approach Using Dye Tracing and Temperature. *Groundwater*, 58(6):924–937.

Bonacci, O. (2001). Analysis of the maximum discharge of karst springs. *Hydrogeology Journal*, 9(4):328–338.

Bresinsky, L., Kordilla, J., Thoenes, E., Würsch, T., Engelhardt, I., and Sauter, M. (2020). Simulating Climate Change Impacts on the Recharge Dynamics of a Mediterranean Karst Aquifer. Technical report.

Burg, A., Yechieli, Y., and Galili, U. (2016). Response of a coastal hydrogeological system to a rapid decline in sea level; the case of Zuqim springs – The largest discharge area along the Dead Sea coast. *Journal of Hydrology*, (536):222–235.

Chen, Z. and Goldscheider, N. (2014). Modeling spatially and temporally varied hydraulic behavior of a folded karst system with dominant conduit drainage at catchment scale, Hochifen–Gottesacker, Alps. *Journal of Hydrology*, 514:41–52.

Diersch, H.-J. G. (2014). *FEFLOW: Finite Element Modeling of Flow, Mass and Heat Transport in Porous and Fractured Media*. Springer Berlin Heidelberg : Imprint: Springer, Berlin, Heidelberg, 1st ed. 2014 edition.

Fahrmeier, N., Frank, S., Goeppert, N., and Goldscheider, N. (2022). Multi-scale characterization of a complex karst and alluvial aquifer system using a combination of different tracer methods. *Hydrogeology Journal*, Accepted Manuscript Draft:33.

Fahrmeier, N., Goeppert, N., and Goldscheider, N. (2021). Comparative application and optimization of different single-borehole dilution test techniques. *Hydrogeology journal*, 29(1):199–211. Publisher: Springer.

Fiasca, B., Stoch, F., Olivier, M.-J., Maazouzi, C., Petitta, M., Di Cioccio, A., and Galassi, D. M. (2014). The dark side of springs: what drives small-scale spatial patterns of subsurface meiofaunal assemblages? *Journal of Limnology*, 73(1):71–80.

Fleury, P., Plagnes, V., and Bakalowicz, M. (2007). Modelling of the functioning of karst aquifers with a reservoir model: Application to Fontaine de Vaucluse (South of France). *Journal of Hydrology*, 345(1-2):38–49.

Ford, D. and Williams, D. (2007). *Karst Hydrogeology and Geomorphology*. John Wiley & Sons Ltd, Chichester.

Frank, S., Goeppert, N., Ohmer, M., and Goldscheider, N. (2019). Sulfate variations as a natural tracer for conduit-matrix interaction in a complex karst aquifer. *Hydrological Processes*, 33(9):1292–1303.

Gargani, J. and Rigollet, C. (2007). Mediterranean Sea level variations during the Messinian salinity crisis. *Geophysical Research Letters*, 34(10):L10405.

Ghasemizadeh, R., Yu, X., Butscher, C., Hellweger, F., Padilla, I., and Alshawabkeh, A. (2015). Equivalent Porous Media (EPM) Simulation of Groundwater Hydraulics and Contaminant Transport in Karst Aquifers. *PLOS ONE*, 10(9):e0138954.

Glennon, A. and Groves, C. (2002). An examination of perennial stream drainage patterns within the Mammoth Cave watershed, Kentucky. *Journal of Cave and Karst Studies 64(1)*, pages 82–91.

Goldscheider, N. (2019). A holistic approach to groundwater protection and ecosystem services in karst terrains. *Carbonates and Evaporites*, 34(4):1241–1249.

Green, R. T., Painter, S. L., Sun, A., and Worthington, S. R. H. (2006). Groundwater Contamination in Karst Terranes. *Water, Air, & Soil Pollution: Focus*, 6(1-2):157–170.

Hartmann, A., Goldscheider, N., Wagener, T., Lange, J., and Weiler, M. (2014). Karst water resources in a changing world: Review of hydrological modeling approaches:. *Reviews of Geophysics*, 52(3):218–242.

Jeannin, P.-Y. (2001). Modeling flow in phreatic and epiphreatic Karst conduits in the Hölloch Cave (Muotatal, Switzerland). *Water Resources Research*, 37(2):191–200.

Kavouri, K. and Karatzas, G. P. (2016). Integrating Diffuse and Concentrated Recharge in Karst Models. *Water Resources Management*, 30(15):5637–5650.

Kiraly, L. (1998). Modelling Karst Aquifers by the Combined Discrete Channel and Continuum Approach. *Bulletin du Centre d'Hydrogeologie*, Vol. 16:77–98.

Kolokotronis, V., Plum, H., Schloz, W., and Rausch, R. (2002). Hydrogeologische Karte von Baden-Württemberg. Ostalb. Erläuterungen. Technical report, Landesamt für Geologie, Rohstoffe und Bergbau Baden-Württemberg; Landesanstalt für Umweltschutz, Baden-Württemberg, Freiburg, Karlsruhe.

Kordilla, J., Sauter, M., Reimann, T., and Geyer, T. (2012). Simulation of saturated and unsaturated flow in karst systems at catchment scale using a double continuum approach. *Hydrology and Earth System Sciences*, 16(10):3909–3923.

Kovács, A. and Sauter, M. (2007). *Modelling karst hydrodynamics. In book: Methods in Karst Hydrogeology*. Taylor and Francis.

Ladouche, B., Marechal, J.-C., and Dorfliger, N. (2014). Semi-distributed lumped model of a karst system under active management. *Journal of Hydrology*, 509:215–230.

Lakušić, S. (2018). Application of artificial neural networks for hydrological modelling in Karst. *Journal of the Croatian Association of Civil Engineers*, 70(1):1–10.

Lauber, U., Ufrecht, W., and Goldscheider, N. (2013). Neue Erkenntnisse zur Struktur der Karstentwässerung im aktiven Höhlensystem des Blautopfs. *Grundwasser*, 18(4):247–257.

Lauber, U., Ufrecht, W., and Goldscheider, N. (2014). Spatially resolved information on karst conduit flow from in-cave dye tracing. *Hydrology and Earth System Sciences*, 18(2):435–445.

Liesch, T., Wunsch, A., Chen, Z., and Goldscheider, N. (2021). Modeling the discharge behavior of an alpine karst spring influenced by seasonal snow accumulation and melting based on a deep-learning approach. other, pico.

Martínez-Santos, P. and Andreu, J. (2010). Lumped and distributed approaches to model natural recharge in semiarid karst aquifers. *Journal of Hydrology*, 388(3-4):389–398.

Ninanya, H., Guiguer, N., Vargas, E. A., Nascimento, G., Araujo, E., and Cazarin, C. L. (2018). Analysis of water control in an underground mine under strong karst media influence (Vazante mine, Brazil). *Hydrogeology Journal*, 26(7):2257–2282.

Paleologos, E. K., Skitzi, I., Katsifarakis, K., and Darivianakis, N. (2013). Neural network simulation of spring flow in karst environments. *Stochastic Environmental Research and Risk Assessment*, 27(8):1829–1837.

Panday, S., Langevin, C., Niswonger, R., Ibaraki, M., and Hughes, J. (2013). *MODFLOW–USG Version 1: An Unstructured Grid Version of MODFLOW for Simulating Groundwater Flow and Tightly Coupled Processes Using a Control Volume Finite-Difference Formulation*, volume book 6, chap. A45. U.S. Geological Survey Techniques and Methods. Series: Techniques and Methods.

Peleg, N. and Gvirtzman, H. (2010). Groundwater flow modeling of two-levels perched karstic leaking aquifers as a tool for estimating recharge and hydraulic parameters. *Journal of Hydrology*, 388(1-2):13–27.

Petitta, M., Caschetto, M., Galassi, D. M. P., and Aravena, R. (2015). Dual-flow in karst aquifers toward a steady discharge spring (Presciano, Central Italy): influences on a subsurface groundwater dependent ecosystem and on changes related to post-earthquake hydrodynamics. *Environmental Earth Sciences*, 73(6):2609–2625.

Scanlon, B. R., Mace, R. E., Barrett, M. E., and Smith, B. (2003). Can we simulate regional groundwater flow in a karst system using equivalent porous media models? Case study, Barton Springs Edwards aquifer, USA. *Journal of Hydrology*, 276(1-4):137–158.

Schloz, W., Armbruster, V., Prestel, R., and Weinzierl, W. (2007). Hydrogeologisches Abschlussgutachten zur Neuabgrenzung des Wasserschutzgebietes Donauried-Hürbe für die Fassungen des Zweckverbandes Landeswasserversorgung im württembergischen Donauried und bei Giengen-Burgberg. Technical report, Landesamt für Geologie Rohstoffe und Bergbau, Regierungspräsidium Freiburg,.

Shi, P., Zhou, M., Qu, S., Chen, X., Qiao, X., Zhang, Z., and Ma, X. (2013). Testing a Conceptual Lumped Model in Karst Area, Southwest China. *Journal of Applied Mathematics*, 2013:1–10.

Shoemaker, W., Kuniansky, E., Birk, S., Bauer, S., and Swain, E. (2008). Documentation of a Conduit Flow Process (CFP) for MODFLOW-2005. Techniques and Methods, U.S. Geological Survey Techniques and Methods. Series: Techniques and Methods.

Udluft, P., editor (2000). *Das Grundwasser im schwäbischen Donautal: hydrologisch-hydrogeologische Untersuchung mit Erstellung eines Grundwassermodells im Maßstab 1: 25 000/50 000 im Donautal zwischen Ulm/Neu-Ulm und Neuburg an der Donau*. Number 11 in Schriftenreihe der Bayerischen Sand- und Kiesindustrie. Bayerischer Industrieverband Steine und Erden, Fachabt. Sand- und Kiesindustrie, München.

Villinger, E. (1977). *Über Potentialverteilung und Strömungssysteme im Karstwasser der Schwäbischen Alb (Oberer Jura, SW-Deutschland)*. Schweizerbart Science Publishers, Stuttgart, Germany.

Villinger, E. and Ufrecht, E. (1989). Ergebnisse neuer Markierungsversuche im Einzugsgebiet des Blautopfs (mittlere Schwaebische Alb). *Mitt. Verb. dt. Hohlen- und Karstforsch*, 35:S. 25–38.